NUMERICAL COMPUTING PARADIGMS FOR THE DYNAMICS OF SQUEEZING RHEOLOGY OF THIRD GRADE FLUID

by

***Saeed Ehsan AWAN*[a], *Muhammad AWAIS*[b], *Abdul QAYYUM*[c], *Saeed Ur REHMAN*[a*], *Ajmal KHAN*[a], *Haider ALI*[d], *and Muhammad Asif Zahoor RAJA*[a,e]**

[a] Department of Electrical and Computer Engineering, COMSATS University Islamabad, Attock Campus, Attock, Pakistan
[b] Department of Mathematics, COMSATS University Islamabad, Attock Campus, Attock, Pakistan
[c] Department of Mathematics, Federal Urdu University of Arts, Science & Technology, Islamabad, Pakistan
[d] Department of Electrical Engineering Technology, University of Technology, Nowshera, Pakistan
[e] Future Technology Research Center, National Yunlin University of Science and Technology, University Road, Section 3, Douliou, Yunlin, Taiwan, R.O.C.

Original scientific paper
https://doi.org/10.2298/TSCI190508160A

In the current study, investigation for the time-dependent flow of third grade fluid between two disks is presented by exploiting the competency of numerical solvers based on Adams and implicit backward difference methods. The applicable mathematical equations are derived and simplified using boundary-layer approach. Transformations are invoked for conversion of PDE to ODE. Numerical treatment is done with Adams and backward difference scheme. The graphical and numerical illustrations are incorporated to present the effect of physical quantities in fluidic system involving squeezing disks. The level of accuracy is achieved with the help of absolute error graph between Adams and Backward difference scheme for each variants of the system model. Validation of the performance on the basis of convergence analysis also presented.

Key words: *fluid dynamics, squeezing flow, third grade fluid, Adams method, implicit backward difference scheme*

Introduction

Non-Newtonian fluids play a key role in several medical as well as engineering fields, specific examples regarding applications of non-Newtonian fluids include bacteriology, bubble columns, polymer solution, food industries, chemical/petroleum, mineral processing industries, *etc*. Several materials *i.e*. shampoo, mud, blood, ketchup, milk, certain oils, polymers *etc*., are non-Newtonian. Hence, the interest in these fluids has specially grown considerably. Such fluids have diverse characteristics in terms of rheological features. Therefore, the shear-stress-strain relationships in non-Newtonian fluids differ greatly from the Newtonian fluid. Researchers mainly used the second grade [1-11]. Flows between disks have been a subject of much interest, as this configuration can be used in rheometer, manufacture of composites and polymers, injection shaping and several others. Researchers [12-21] have presented

* Corresponding author, e-mail: saeedurrehman@ciit-attock.edu.pk

several studies regarding such flows and discussed their applications in detail. The goal of this communication is to address the time-dependent flow of third grade fluid between disks. The novel aspects of shear thinning/thickening of various materials in nature cannot be described by second grade fluids. Hence one requires another fluid model exhibiting such model features. The extra rheological parameters in the third-grade fluid yields more complicated and non-linear equation than the second-grade fluid. The real motivation in this study is twofold. Firstly, to explore the shear thinning/shear thickening effects. Secondly to develop the convergent numerical solution to more non-linear problem. Analysis regarding important parameters in the solution is made.

Salient features of the proposed scheme are highlighted briefly as:

- The time-dependent flow of third grade fluid is presented with rich dynamical analysis of the model by mean of shear thinning/shear thickening property which cannot perceive in second grad fluids
- Transformation procedure reduces the stiff non-linear partial differential system of the original model to relatively simple higher non-linear order ordinary differential system.
- The graphical and numerical illustrations established the worth of numerical solvers to study the influence of sundry physical quantities in the fluidic system involving squeezing disks.
- The level of accuracy achieved by the proposed numerical procedure is demonstrated with the help of absolute error graph between Adams and backward difference (BDF) for each variants of the system model.
- Validation of the performance on the basis of convergence analysis is also performed.

Analysis

Let us consider the rheology of third grade fluid having separation between the walls as $H(1-at)^{1/2}$, with upper disk at $z = h(t) = H(1-at)^{1/2}$ is moving with velocity $-aH/2(1-at)^{1/2}$ while, the lower is fixed. The equations presenting the fluid rheology are:

$$\frac{\partial u}{\partial r}+\frac{u}{r}+\frac{\partial w}{\partial z}=0 \tag{1}$$

$$\begin{aligned}&\frac{\partial u}{\partial t}+u\frac{\partial u}{\partial r}+w\frac{\partial u}{\partial z}=-\frac{1}{\rho}\frac{\partial p}{\partial r}+\nu\left(\frac{\partial^2 u}{\partial r^2}+\frac{\partial^2 u}{\partial z^2}+\frac{1}{r}\frac{\partial u}{\partial r}-\frac{u}{r^2}\right)+\\
&+\frac{\alpha_1}{\rho}\left[\begin{array}{c}2\frac{\partial^3 u}{\partial t\partial r^2}+\frac{2}{r}\frac{\partial^2 u}{\partial t\partial r}+\frac{\partial^3 u}{\partial t\partial z^2}+\frac{\partial^3 w}{\partial z\partial t\partial r}+u\left(2\frac{\partial^3 u}{\partial r^3}+\frac{2}{r}\frac{\partial^2 u}{\partial r^2}+\frac{\partial^3 u}{\partial r\partial z^2}+\frac{\partial^3 w}{\partial z\partial r^2}\right)+\\
+w\left(2\frac{\partial^3 u}{\partial z\partial r^2}+\frac{2}{r}\frac{\partial^2 u}{\partial z\partial r}+\frac{\partial^3 u}{\partial z^3}+\frac{\partial^3 w}{\partial r\partial z^2}-\frac{2}{r}\frac{\partial u}{\partial z}\right)+\frac{\partial u}{\partial z}\left(3\frac{\partial^2 w}{\partial r^2}+4\frac{\partial^2 u}{\partial r\partial z}+\frac{\partial^2 w}{\partial z^2}\right)+\\
+\frac{\partial u}{\partial r}\left(10\frac{\partial^2 u}{\partial r^2}+3\frac{\partial^2 u}{\partial z^2}+\frac{\partial^2 w}{\partial r\partial z}+\frac{4}{r}\frac{\partial u}{\partial r}-\frac{2u}{r^2}\right)+\frac{\partial w}{\partial z}\left(2\frac{\partial^2 u}{\partial z^2}+\frac{\partial^2 w}{\partial z\partial r}\right)-\\
-\frac{2}{r^2}\frac{\partial u}{\partial t}+\frac{\partial w}{\partial r}\left(2\frac{\partial^2 u}{\partial z\partial r}+4\frac{\partial^2 w}{\partial r^2}+2\frac{\partial^2 u}{\partial z\partial r}+\frac{2}{r}\left(\frac{\partial u}{\partial z}+\frac{\partial w}{\partial r}\right)+3\frac{\partial^2 w}{\partial z^2}+\frac{\partial^2 u}{\partial r\partial z}\right)\end{array}\right]+\end{aligned}$$

$$+\frac{\alpha_2}{\rho}\left[\begin{array}{l}\frac{\partial u}{\partial r}\left(8\frac{\partial^2 u}{\partial r^2}+\frac{4}{r}\frac{\partial u}{\partial r}+2\frac{\partial^2 u}{\partial z^2}+2\frac{\partial^2 w}{\partial z\partial r}\right)+\frac{\partial w}{\partial r}\left(4\frac{\partial^2 u}{\partial r\partial z}+2\frac{\partial^2 w}{\partial r^2}+2\frac{\partial^2 w}{\partial z^2}+\frac{1}{r}\frac{\partial w}{\partial r}\right)+\\+\frac{\partial u}{\partial z}\left(4\frac{\partial^2 u}{\partial r\partial z}+2\frac{\partial^2 w}{\partial r^2}+2\frac{\partial^2 w}{\partial z^2}+\frac{1}{r}\frac{\partial u}{\partial z}+\frac{2}{r}\frac{\partial w}{\partial r}\right)+2\frac{\partial w}{\partial z}\left(\frac{\partial^2 u}{\partial z^2}+\frac{\partial^2 w}{\partial r\partial z}\right)-\frac{4u^2}{r^3}\end{array}\right]+$$

$$+\frac{\beta_3}{\rho}\left\{\begin{array}{l}2\frac{\partial u}{\partial r}\left(4\frac{\partial u}{\partial z}\frac{\partial^2 u}{\partial r\partial z}+\frac{8u}{r^2}\frac{\partial u}{\partial r}-\frac{8u^2}{r^3}\right)\left(\frac{2}{r}\frac{\partial u}{\partial r}+\frac{\partial^2 u}{\partial z^2}-\frac{4u}{r^2}\right)\cdot\\ \cdot\left[4\left(\frac{\partial u}{\partial r}\right)^2+2\left(\frac{\partial u}{\partial z}\right)^2+4\left(\frac{\partial w}{\partial z}\right)^2+\frac{4u^2}{r^2}\right]+\\+\frac{\partial u}{\partial z}\left(8\frac{\partial u}{\partial r}\frac{\partial^2 u}{\partial r\partial z}+4\frac{\partial u}{\partial z}\frac{\partial^2 u}{\partial z^2}+8\frac{\partial w}{\partial z}\frac{\partial^2 w}{\partial z^2}++\frac{8u}{r^2}\frac{\partial u}{\partial z}\right)\end{array}\right\} \tag{2}$$

$$\frac{\partial w}{\partial t}+u\frac{\partial w}{\partial r}+w\frac{\partial w}{\partial z}=-\frac{1}{\rho}\frac{\partial p}{\partial z}+\nu\left(\frac{\partial^2 w}{\partial r^2}+\frac{\partial^2 w}{\partial z^2}+\frac{1}{r}\frac{\partial w}{\partial r}\right)+$$

$$+\frac{\alpha_1}{\rho}\left[\begin{array}{l}\frac{\partial^3 w}{\partial t\partial r^2}+\frac{\partial^3 w}{\partial t\partial z^2}+\frac{1}{r}\frac{\partial^2 w}{\partial t\partial r}+\frac{\partial u}{\partial r}\left(4\frac{\partial^2 u}{\partial r\partial z}+2\frac{\partial^2 w}{\partial r^2}+\frac{3}{r}\frac{\partial u}{\partial z}+\frac{1}{r}\frac{\partial w}{\partial r}\right)+\\+u\left(\frac{\partial^3 u}{\partial r^2\partial z}+\frac{\partial^3 w}{\partial r^3}+\frac{1}{r}\frac{\partial^2 u}{\partial r\partial z}+\frac{1}{r}\frac{\partial^2 w}{\partial r^2}+2\frac{\partial^3 w}{\partial r\partial z^2}\right)+\\+w\left(\frac{\partial^3 w}{\partial r\partial z^2}+\frac{1}{r}\frac{\partial^2 w}{\partial r\partial z}+\frac{\partial^3 w}{\partial z^3}\right)+\frac{\partial w}{\partial r}\left(3\frac{\partial^2 u}{\partial z^2}+4\frac{\partial^2 w}{\partial r\partial z}+\frac{\partial^2 u}{\partial r^2}+\frac{2}{r}\frac{\partial w}{\partial z}\right)+\\+\frac{\partial u}{\partial z}\left(3\frac{\partial^2 u}{\partial r^2}+3\frac{\partial^2 w}{\partial z\partial r}+2\frac{\partial^2 w}{\partial r\partial z}+4\frac{\partial^2 u}{\partial z^2}\right)+\frac{\partial w}{\partial z}\left(3\frac{\partial^2 w}{\partial r^2}+\frac{1}{r}\frac{\partial w}{\partial r}+9\frac{\partial^2 w}{\partial z^2}\right)\end{array}\right]+$$

$$+\frac{\alpha_2}{\rho}\left[\begin{array}{l}\frac{\partial u}{\partial r}\left(2\frac{\partial^2 w}{\partial r^2}+2\frac{\partial^2 u}{\partial r\partial z}+\frac{2}{r}\frac{\partial u}{\partial z}+\frac{2}{r}\frac{\partial w}{\partial r}\right)+\frac{\partial u}{\partial z}\left(2\frac{\partial^2 u}{\partial r^2}+4\frac{\partial^2 w}{\partial r\partial z}+2\frac{\partial^2 u}{\partial z^2}\right)+\\+\frac{\partial w}{\partial r}\left(2\frac{\partial^2 u}{\partial r^2}+4\frac{\partial^2 w}{\partial r\partial z}+2\frac{\partial^2 u}{\partial z^2}\right)+2\frac{\partial w}{\partial z}\left(\frac{\partial^2 w}{\partial r^2}+3\frac{\partial^2 w}{\partial z^2}+\frac{1}{r}\frac{\partial w}{\partial r}\right)\end{array}\right]+$$

$$+\frac{\beta_3}{\rho}\left\{\begin{array}{l}\left(\frac{\partial u}{\partial z}+\frac{\partial w}{\partial r}\right)\left[8\frac{\partial u}{\partial r}\frac{\partial^2 u}{\partial r^2}+8\frac{\partial w}{\partial z}\frac{\partial^2 w}{\partial r\partial z}+4\left(\frac{\partial u}{\partial z}+\frac{\partial w}{\partial r}\right)\left(\frac{\partial^2 u}{\partial r\partial z}+\frac{\partial^2 w}{\partial r^2}\right)+\frac{8u}{r^2}\frac{\partial u}{\partial r}-\frac{8u^2}{r^3}\right]+\\+\left(\frac{1}{r}\frac{\partial w}{\partial r}+\frac{\partial^2 w}{\partial r^2}+\frac{\partial^2 w}{\partial z^2}\right)\left[4\left(\frac{\partial u}{\partial r}\right)^2+2\left(\frac{\partial u}{\partial z}+\frac{\partial w}{\partial r}\right)^2+4\left(\frac{\partial w}{\partial z}\right)^2+\frac{4u^2}{r^2}\right]+\\+2\frac{\partial w}{\partial z}\left[8\frac{\partial u}{\partial r}\frac{\partial^2 u}{\partial r\partial z}+4\left(\frac{\partial u}{\partial z}+\frac{\partial w}{\partial r}\right)\left(\frac{\partial^2 u}{\partial z^2}+\frac{\partial^2 w}{\partial z\partial r}\right)+8\frac{\partial w}{\partial z}\frac{\partial^2 w}{\partial z^2}+\frac{8u}{r^2}\frac{\partial u}{\partial z}\right]\end{array}\right\} \tag{3}$$

Equations (2) and (3) represents the components of law of conservation of momentum. In this analysis we have considered the third grade non Newtonian fluid model which is more general model as compared to Newtonian model. For $\alpha_1 = \alpha_2 = \beta_3$ the current equation is reduced to the component of law of conservation of momentum for Newtonian model.

The associated boundary conditions are:

$$\begin{gathered} u=0, \quad w=\frac{\partial h}{\partial t}, \quad \text{at} \quad z=h(t) \\ u=0, \quad w=-w_0, \quad \text{at} \quad z=0 \end{gathered} \tag{4}$$

Utilizing:

$$u=\frac{ar}{2(1-at)}f'(\eta), \quad w=-\frac{aH}{\sqrt{1-at}}f(\eta), \quad \eta=\frac{z}{H\sqrt{1-at}} \tag{5}$$

By simplification we reach:

$$\begin{gathered} f^{(\text{iv})}-S_q\left(\eta f'''+3f''-2ff'''\right)+\frac{\varepsilon_1}{2}\left[f^{(\text{v})}+5f^{(\text{iv})}-4f''f'''-2f'f^{(\text{iv})}-2ff^{(\text{v})}\right]- \\ -\frac{\varepsilon_2}{2}\left[2f'f^{(\text{iv})}+4f''f'''\right]+\varepsilon_3\left\{\begin{array}{c}\varepsilon_4\left[\frac{3}{2}(f''')^2f^{(\text{iv})}+3f''(f''')^2\right]+ \\ +6(f')^2f^{(\text{iv})}+48f'f''f'''+14(f'')^3\end{array}\right\}=0 \end{gathered} \tag{6}$$

$$\begin{gathered} f\to S, \quad f'\to 0, \quad \text{at} \quad \eta=0 \\ f\to 0.5, \quad f'\to 0, \quad \text{at} \quad \eta=1 \end{gathered} \tag{7}$$

In which the dimensionless quantities are

$$S_q=\frac{aH^2}{2\nu}, \quad \varepsilon_1=\frac{a\alpha_1}{\mu(1-at)}, \quad \varepsilon_2=\frac{a\alpha_2}{\mu(1-at)}, \quad \varepsilon_3=\frac{a^2\beta_3}{\mu(1-at)^2}, \quad \varepsilon_4=\frac{r^2}{H^2(1-at)} \tag{8}$$

Note that if we put $\varepsilon_3 = 0$ and $\varepsilon_2 = -\varepsilon_1$ in eq (6) then eq. (6) reduces to second grade fluid [21]. Moreover skin friction is:

$$C_{fr}=\frac{\tau_{rz}\big|_{z=h(t)}}{\rho\left[\dfrac{aH}{2\sqrt{1-at}}\right]^2} \tag{9}$$

with

$$\begin{gathered} \tau_{rz}=\mu\left(\frac{\partial u}{\partial z}+\frac{\partial w}{\partial r}\right)+\alpha_1\left[\begin{array}{c}\dfrac{\partial^2 u}{\partial t\partial z}+\dfrac{\partial^2 w}{\partial t\partial r}+u\left(\dfrac{\partial^2 u}{\partial r\partial z}+\dfrac{\partial^2 w}{\partial r^2}\right)+w\left(\dfrac{\partial^2 u}{\partial z^2}+\dfrac{\partial^2 w}{\partial z\partial r}\right)+ \\ \dfrac{\partial u}{\partial r}\left(3\dfrac{\partial u}{\partial z}+\dfrac{\partial w}{\partial r}\right)+\dfrac{\partial w}{\partial z}\left(\dfrac{\partial u}{\partial z}+3\dfrac{\partial w}{\partial r}\right)\end{array}\right]+ \\ +\alpha_2\left[2\frac{\partial u}{\partial r}\left(\frac{\partial u}{\partial z}+\frac{\partial w}{\partial r}\right)+2\frac{\partial w}{\partial z}\left(\frac{\partial u}{\partial z}+\frac{\partial w}{\partial r}\right)\right]+ \\ +\beta_3\left(\frac{\partial u}{\partial z}+\frac{\partial w}{\partial r}\right)\left[4\left(\frac{\partial u}{\partial r}\right)^2+2\left(\frac{\partial u}{\partial z}+\frac{\partial w}{\partial r}\right)^2+4w\left(\frac{\partial w}{\partial z}\right)^2+\frac{4u^2}{r^2}\right] \end{gathered} \tag{10}$$

Dimensionless form of eq. (9) is:

$$\frac{H^2}{r^2} R_{er} C_{fr} = \left[1 + \frac{3}{2}\varepsilon_1 + \frac{1}{2}\varepsilon_3 \varepsilon_4 f''(1)\right] f''(1) \tag{11}$$

where

$$R_{er}^{-1} = \frac{2\nu}{raH\sqrt{1-at}} \tag{12}$$

we solved the non-linear system.

Numerical solutions: Adams and backward difference method

The competency of Adams numerical solver along with BDF method [22-26] is also utilized to solve the system given in eq. (6) and boundary conditions as given:

$$\begin{gathered} f \to S, \quad f' \to 0, \quad \text{at} \quad \eta = 0 \\ f \to 0.5, f' \to 0, \quad f'' \to 1, \quad \text{at} \quad \eta = 1 \end{gathered} \tag{13}$$

In Adam predictor-corrector method, we first predict the solution and in next stage accurate solution is achieved through corrector. Consider the eq. (6) for velocity profile as:

$$\frac{\mathrm{d}f}{\mathrm{d}\eta} = s(\eta, f), \quad f(\eta_0) = f_0 \tag{14}$$

Two Step Adam Predictor relation for velocity profile will be:

$$f_{m+1} = f_m + \frac{h}{2}\left[3s(\eta_m, f_m) - s(\eta_{m-1}, f_{m-1})\right] \tag{15}$$

While two step Adam corrector formula for velocity profile will be:

$$f_{m+1} = f_m + \frac{h}{2}\left[s(\eta_{m+1}, f_{m+1}) - s(\eta_m, f_m)\right] \tag{16}$$

To solve the ODE eq. (6) along with boundary conditions given in eq. (7), the Adam numerical solver and implicit BDF methods are applied by invoking the *NDSolve* built-in routine of BDF Mathematica software package with default settings. The dynamics of the problem is analysis by comparing the results of both methods.

Numerical experimentation with discussion

The aim of current portion is to describe the behavior of physical quantities on velocity profile of the fluid. Figure 1(a) portrays the effects of on the flow profiles. It is noted that the velocity field f' increases for η between 0 and 0.7 while decreases for η between 0.7 and 1 with the increment in ε_1. Opposite behavior of the flow has observed near to the lower plate. Figure 1(b) shows the error analysis for different values of ε_1 which shows that error is negligible in the computed results. The effects of ε_2 on the flow profile and error analysis are presented in figs. 2(a) and 2(b). It is observed that flow field decreases with an increase in ε_2. Moreover, the error for different values of ε_2 is quite negligible. The effects of ε_4 on the flow field are portrayed in fig. 3(a). It is quite evident that the velocity field and momentum boundary-layer are decreasing functions of ε_4. Figure 3(b) shows that error in results for different values of ε_4 are negligible. Figures 4(a) and 4(b) portray the effects of S on the flow field and

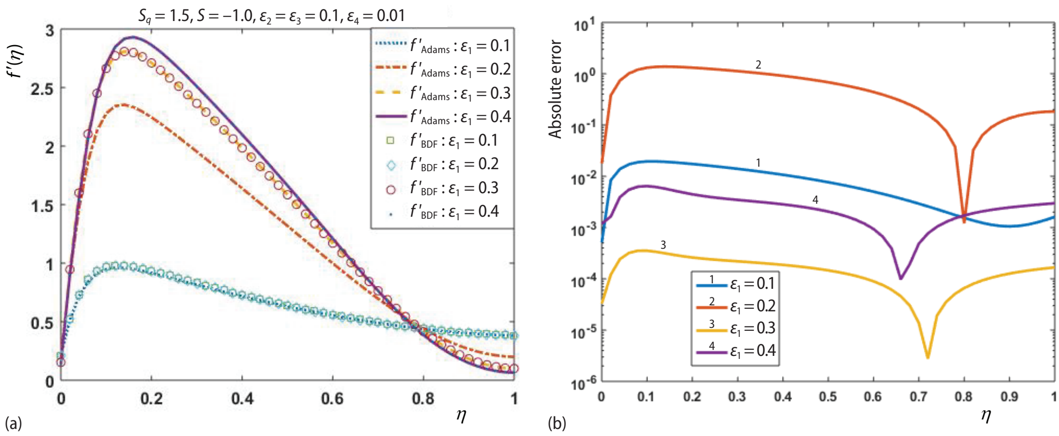

Figure 1. Influence of variation in ε_1 on $f'(\eta)$; (a) comparison of results and (b) magnitude of the absolute error

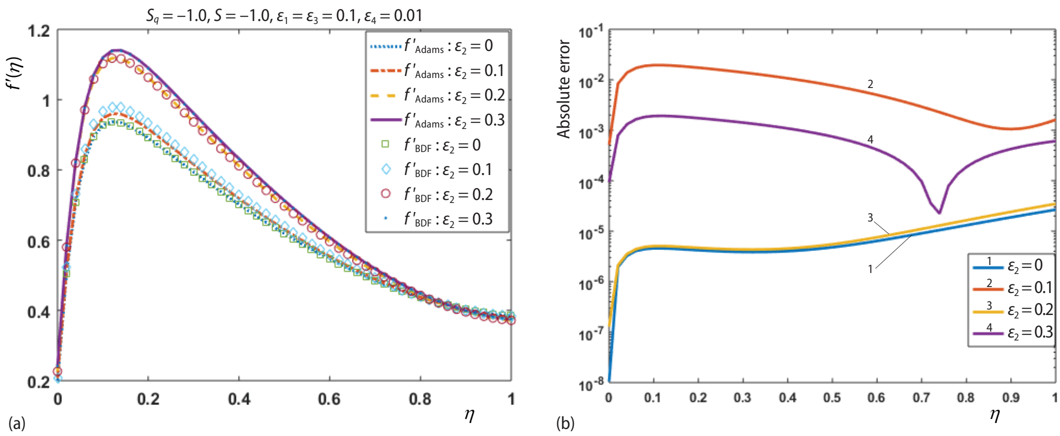

Figure 2. Influence of variation in ε_2 on $f'(\eta)$; (a) comparison of results and (b) magnitude of the absolute error

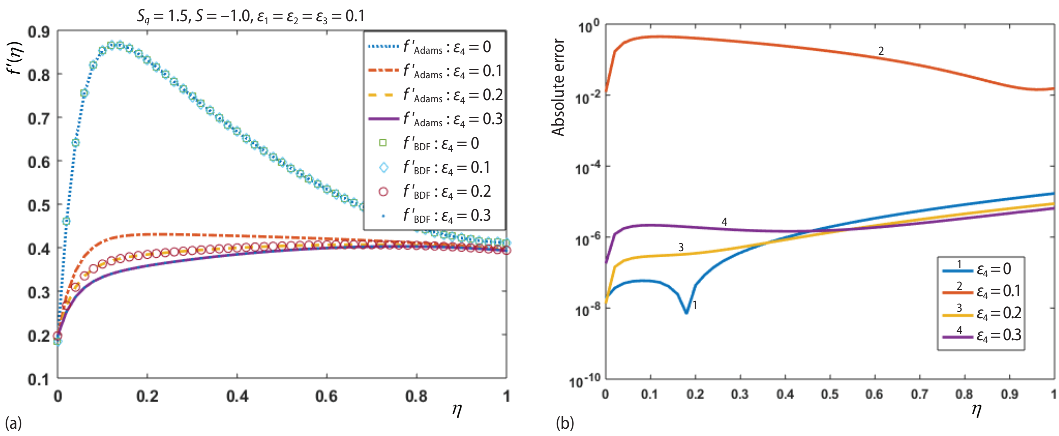

Figure 3. Influence of variation in ε_4 on $f'(\eta)$; (a) comparison of results and (b) magnitude of the absolute error

the error computation for different values of S. It is evident that due to increment in S will tend to increase velocity profile since suction is a boosting agent which enhance the flow. Moreover, it is also noted that error for different values of S is negligible fig. 4(b). Figure 5(a) portrays the effects of squeezing phenomenon on the flow profile. It is noticed that velocity increases with an increment in the squeezing process. Moreover, it is further noted the error for different values of squeezing process is negligible fig. 5(b). The numerical magnitude of skin friction coefficient for different physical quantities are listed in tab. 1. The results presented in tab. 1 show that values of the skin friction coefficient increases with an increment in S while decreases by increments in both of S_q and ε_3. Computational complexity and convergence analysis for squeezing parameter is presented in tab. 2. It is observed that all five numerical techniques are suitable for both non stiff as well as stiff and accuracy goal is achieved for squeezing parameter variation of third grade fluidic model which proves the convergence and stability of numerical methods.

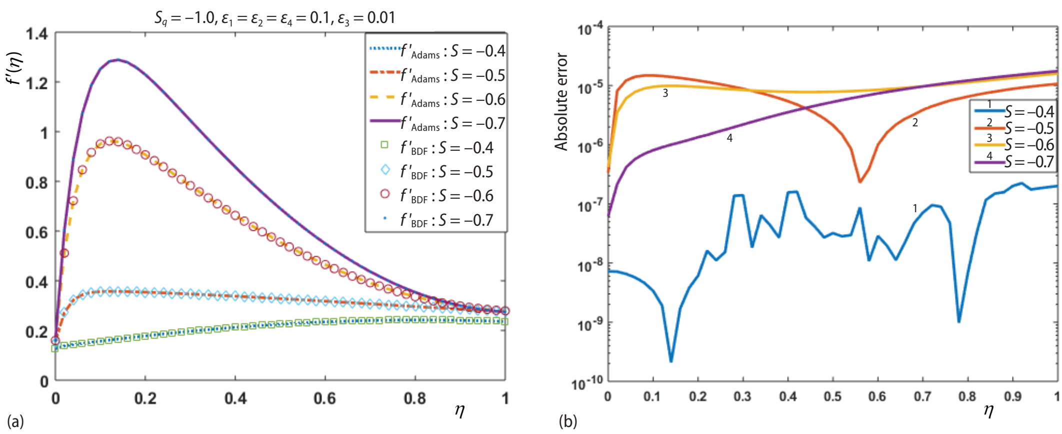

Figure 4. Influence of variation in S on $f'(\eta)$; (a) comparison of results and (b) magnitude of the absolute error

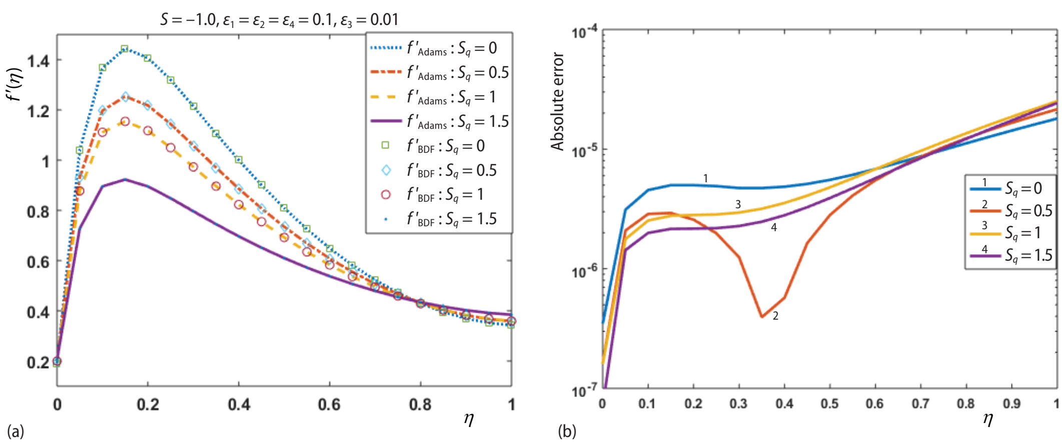

Figure 5. Influence of variation in S_q on $f'(\eta)$; (a) comparison of results and (b) magnitude of the absolute error

Table 1. Skin friction coefficients $(H^2/r^2)R_{er}C_{fr}$ for different values of emerging parameters $\varepsilon_1 = \varepsilon_2 = \varepsilon_4 = 0.1$

S	S_q	ε_3	$\frac{H^2}{r^2}R_{er}C_{fr}$
–1.5	2.0	0.01	–23.97831
–1.0	2.0	0.01	–15.84972
–0.5	2.0	0.01	–9.073212
.0	2.0	0.01	–3.870458
–1.0	0.0	0.01	–12.10583
–1.0	1.0	0.01	–14.03073
–1.0	2.0	0.01	–15.84972
–1.0	2.5	0.01	–16.70936
–1.0	2.0	0.0	–15.07652
–1.0	2.0	0.01	–15.84972
–1.0	2.0	0.02	–16.15729
–1.0	2.0	0.03	–16.25819

Table 2. Convergence and complexity measures of the system in case of $S_q = 0.5$

Method	Accuracy goal	Timing	Steps	Evaluation
Adams	10^{-20}	8.25	205	428
	10^{-15}	7.5625	199	419
	10^{-10}	6.34375	178	367
	10^{-5}	4.75	131	265
BDF*	10^{-20}	46.9688	405	497
	10^{-15}	40.1719	392	490
	10^{-10}	22.6094	354	425
	10^{-5}	12.7813	213	252
ERK**	10^{-20}	25.3125	48	654
	10^{-15}	19.5625	44	648
	10^{-10}	13.5313	40	641
	10^{-5}	7.48438	28	449
IRK***	10^{-20}	40.5469	84	1397
	10^{-15}	37.7813	81	1393
	10^{-10}	29.375	80	1390
	10^{-5}	25.625	63	1075
ET****	10^{-20}	20.9063	24	718
	10^{-15}	17.3594	22	710
	10^{-10}	13.1719	18	704
	10^{-5}	8.76563	16	512

* Backward difference method

** stands for Explicit Runge Kutta

*** stands for Implicit Runge Kutta

**** stands for Extrapolation

Conclusion

On the basis of simulation performed through numerical procedures for squeezing flow model following inferences are drawn as follows.

- Squeezing effects have opposite behavior near channel walls.
- Suction effect has dominant behavior at the central portal of channel.
- Skin friction increases with an increase in third grade parameter.
- The effects of squeezing parameters on the velocity profile of the fluid are inverse behavior in case of both the suction and the blowing.
- Error graphs show that the results have negligible error. Precession of 7 to 8 decimal places of accuracy is consistently observed for each scenario.
- It can be seen that all five numerical methods are applicable for both non-stiff, *i. e.*, 10^{-05} and 10^{-10}, as well as stiff, *i. e.*, 10^{-15} and 10^{-20} accuracy goals for all four variation of the fluidic model, which established the stability and convergence of the numerical procedures.

In future one may explore in stochastic numerical methods [27-29] based on artificial intelligence algorithms, *i. e.*, neural networks, genetic algorithm, particle swarm optimization, backtracking search optimization, fractional evolutionary and swarming techniques, for solutions of non-linear squeezing fluidics models for a very limited class of solvers are available for numerical treatment.

References

[1] Fetecau, C., Fetecau, C., Starting Solutions for the Motion of a Second Grade Fluid Due to Longitudinal and Torsional Oscillations of a Circular Cylinder, *International Journal of Engineering Science., 44* (2006), 11-12, pp.788-796
[2] Jamil, M., *et al.,* Helical Flows of Second Grade Fluid Due to Constantly Accelerated Shear Stresses, *Communications in Nonlinear Science and Numerical Simulation, 16* (2011), 4, pp. 1959-1969
[3] Hayat, T., *et al.,* Thermal-Diffusion and Diffusion-Thermo Effects on Axisymmetric Flow of a Second Grade Fluid, *International Journal of Heat and Mass Transfer, 54* (2011), 13-14, pp. 3031-3041
[4] Tan, W., Masuoka, T., Stokes First Problem for a Second Grade Fluid in a Porous Half-Space with Heated Boundary, *International Journal of Non-Linear Mechanics, 40* (2005), 4, pp.515-522
[5] Khan, A. A., *et al.,* Effects of Chemical Reaction on Third-Grade MHD Fluid Flow Under the Influence of Heat and Mass Transfer with Variable Reactive Index, *Heat Transfer Research, 50* (2019), 11, pp. 1061-1080
[6] Ahmad, A., Asghar, S., Flow of a Second Grade Fluid over a Sheet Stretching with Arbitrary Velocities Subject to a Transverse Magnetic Field, *Applied Mathematics Letters, 24* (2011), 11, pp.1905-1909
[7] Okoya, S. S., Computational Study of Thermal Influence in Axial Annular Flow of a Reactive Third Grade Fluid with Non-Linear Viscosity, *Alexandria Engineering Journal, 58* (2019), 1, pp. 401-411
[8] Shafiq, A., *et al.,* Significance of Double Stratification in Stagnation Point Flow of Third-Grade Fluid Towards a Radiative Stretching Cylinder, *Mathematics, 7* (2019), 11, 1103
[9] Hayat, T., Awais, M., Simultaneous Effects of Heat and Mass Transfer on Time-Dependent Flow over a Stretching Surface, *International Journal for Numerical Methods in Fluids, 67* (2011), 11, pp. 1341-1357
[10] Hayat, T., *et al.,* Unsteady Three-Dimensional Flow in a Second-Grade Fluid over a Stretching Surface, *Zeitschrift für Naturforschung A, 66* (2011), 10-11, pp. 635-642
[11] Fetecau, C., Fetecau, C., *et al.,* General Solutions for the Unsteady Flow of Second-Grade Fluids over an Infinite Plate that Applies Arbitrary Shear to the Fluid, *Zeitschrift für Naturforschung A, 66* (2011), 12, pp. 753-759
[12] Sajid, M., *et al.,* A theoretical Analysis of Blade Coating for Third-Grade Fluid, *Journal of Plastic Film & Sheeting, 35* (2019), 3, pp. 218-238
[13] Khan, Z., *et al.,* Effect of Thermal Radiation and MHD on Non-Newtonian Third Grade Fluid in Wire Coating Analysis with Temperature Dependent Viscosity, *Alexandria Engineering Journal, 57* (2018), 3, pp. 2101-2112

[14] Bilal, S., *et al.,* Heat and Mass Transfer in Hydromagnetic Second-Grade Fluid Past a Porous Inclined Cylinder under the Effects of Thermal Dissipation, *Diffusion and Radiative Heat Flux. Energies, 13* (2020), 1, 278
[15] Hayat, T., *et al.*, Impact of Temperature Dependent Heat Source and Nonlinear Radiative Flow of Third Grade Fluid with Chemical Aspects, *Thermal Science, 24* (2020), 2B, pp. 1173-1182
[16] Sahoo, B., Do, Y., Effects of Slip on Sheet-Driven Flow and Heat Transfer of a Third Grade Fluid Past a Stretching Sheet, *International Communications in Heat and Mass Transfer, 37* (2010) 8, pp. 1064-1071
[17] Abbasbandy, S., Hayat, T., On Series Solution for Unsteady Boundary Layer Equations in a Special Third Grade Fluid, *Communications in Nonlinear Science and Numerical Simulation, 16* (2011), 8, pp. 3140-3146
[18] Awais, M., *et al.,* Hydro Magnetic Falkner-Skan Fluid Reheolgy with Heat Transfer Properties, *Thermal Science, 24* (2020), 1A, pp. 339-346
[19] Siddiqa, S., *et al.,* Thermal Radiation Therapy of Biomagnetic Fluid Flow in the Presence of Localized Magnetic Field, *International Journal of Thermal Sciences, 132*, (2018), Oct., pp. 457-465
[20] Awan, S. E., *et al.,* Dynamical Analysis for Nanofluid Slip Rheology with Thermal Radiation, Heat Generation/Absorption and Convective Wall Properties, *AIP Advances, 8* (2018), 7, 075122
[21] Hayat, T., *et al.,* MHD Squeezing Flow of Second/Grade Fluid between Two Parallel Disks, *International Journal for Numerical Methods in Fluids, 69* (2012), 2, pp. 399-410
[22] Awais, M., *et al.,* Numerical and Analytical Approach for Sakiadis Rheology of Generalized Polymeric Material with Magnetic Field and Heat Source/Sink, *Thermal Science, 24* (2020), 2B, pp. 1183-1194
[23] Awan, S. E., *et al.,* Numerical Treatment for Hydro-Magnetic Unsteady Channel Flow of Nanofluid with Heat Transfer, *Results in Physics, 9* (2018), June, pp. 1543-1554
[24] Awais, M., *et al.,* Nanoparticles and Nonlinear Thermal Radiation Properties in the Rheology of Polymeric Material, *Results in physics, 8* (2018), Mar., pp. 1038-1045
[25] Awais, M., *et al.,* Hydromagnetic Mixed Convective Flow over a Wall with Variable Thickness and Cattaneo-Christov Heat Flux Model: OHAM Aanalysis, *Results in Physics, 8* (2018), Mar., pp. 621-627
[26] Awais, M., *et al.,* Generalized Magnetic Effects in a Sakiadis Flow of Polymeric Nano-Liquids: Analytic and Numerical Solutions, *Journal of Molecular Liquids, 241* (2017), Sept., pp. 570-576
[27] Raja, M. A. Z., *et al.,* Bio-Inspired Computational Heuristics for Sisko Fluid Flow and Heat Transfer Models, *Applied Soft Computing, 71* (2018), Oct., pp. 622-648
[28] Khan, J. A., Raja, M. A. Z., *et al.,* Design and Application of Nature Inspired Computing Approach for Nonlinear Stiff Oscillatory Problems, *Neural Computing and Applications, 26* (2015), 7, pp. 1763-1780
[29] Mehmood, A., *et al.,* Integrated Intelligent Computing Paradigm for the Dynamics of Micropolar Fluid Flow with Heat Transfer in a Permeable Walled Channel, *Applied Soft Computing, 79* (2019), June, pp. 139-162

Paper submitted: May 8, 2019
Paper revised: March 27, 2020
Paper accepted: April 1, 2020

© 2020 Society of Thermal Engineers of Serbia
Published by the Vinča Institute of Nuclear Sciences, Belgrade, Serbia.
This is an open access article distributed under the CC BY-NC-ND 4.0 terms and conditions